Permanent-magnet variable-reluctance linear motor control

I.A. Viorel and L. Szabo

The permanent-magnet variable reluctance linear motors are well suited for precise linear positioning at high speed. In the open-loop drive mode the phase excitation sequence is executed at a given frequency. There is always the peril of losing the synchronism and to affect, this way, motor's performances. The positioning capabilities and dynamic performances of the motor are improved by operating under closed-loop control. In the paper, the control basics are established and detailedly analyzed. By means of computer simulation, the motor characteristics are given in open-loop and closed-loop driving modes. These characteristics stand by to sustain theoretical results and to confirm the validity of the proposed control strategy.

1. Introduction

In numerous branches (as robotics, computer peripheral, NC machine-tools, Computer Aided Manufacturing etc.) - using ultraprecision techniques at high speeds - linear positioning can be realized by *permanent-magnet variable-reluctance linear motors*. These motors offer many advantages such as high speed, accurate positioning, high servo stiffness, smooth travel at all speeds and fast settling times [1].

The permanent-magnet variable-reluctance linear motor is operating under the combined principles of the permanent magnet and variable reluctance. The basic construction of the motor is very simple.

In the open-loop drive mode, the phase excitation sequence is executed at a given frequency, existing a peril of losing the synchronism. The positioning capabilities and dynamic performance of the motor can be improved by operating under closed-loop control. The control system has to offer the possibility to maintain a prescribed motor speed not depending of the load in certain limits. The operating frequency is variable and depends only on the motor capability to realize a certain displacement under given conditions as load and input source limits.

In the paper, under certain simplifying assumptions, which do not affect basically the results, the total tangential force is expressed. Then, the optimum control angle is determined by imposing a maximum value for the average total tangential force developed during a control sequence. The induced e.m.f. computed in both control coils, one excited and the second not supplied, depends on mover's velocity and angular displacement, if the permanent magnet m.m.f. and control-coil amperturns are considered constant. These two e.m.f.s can be utilized in the closed-loop system to estimate the velocity and angular displacement in order to assure the desired control. Finally, by computer simulation, based on a circuit-field coupled model, the motor characteristics are given in open-loop and closed-loop driving modes.

The authors expect that the control basics presented in this paper will provide reliable tools in controlling permanent-magnet variable-reluctance linear motor.

2. Permanent-magnet variable-reluctance linear motors

The permanent-magnet variable-reluctance linear motor, shown in Fig. 1, is a variable-reluctance, permanent-magnet excited synchronous motor having a movable armature (the mover) suspended over a fixed stator (the platen). The platen is an equidistantly toothed bar of any length fabricated from high-permeability cold-rolled steel. The mover consists of two electromagnets having command coils and a permanent magnet between them, which serves as a bias source. Each electromagnet has two poles, and all poles have the same number of teeth. The toothed structure in both parts (mover and platen) has the same very fine

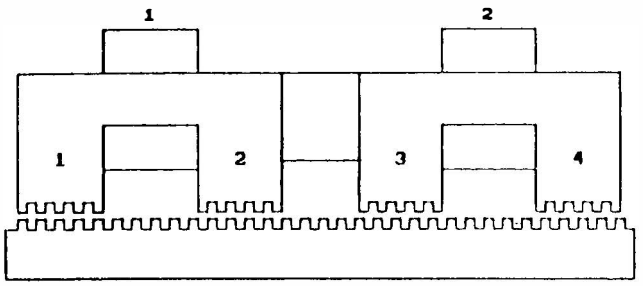

Fig. 1. Four-pole permanent-magnet variable-reluctance linear motor (poles 1÷4; control coils 1,2).

tooth-pitch. Each of the two poles of one electromagnet are displaced with respect to the platen slotting by half of a tooth-pitch. The right-side electromagnet, numbered 2 in Fig. 1, is placed by a multiple of quarter tooth-pitch with respect to electromagnet 1.

The permanent-magnet variable-reluctance linear motor is operating under the combined principles of variable reluctance (tending to move towards the aligned-teeth position in which magnetic reluctance is minimum) and of permanent magnet (having long-life excitation).

The permanent-magnet flux passes through the two electromagnet cores, air-gap and platen. By commutating the permanent magnet flux in a way to concentrate it into a single pole is resulting in a tangential force, which tends to align the teeth of that pole with the platen teeth in a manner as to minimize the air-gap magnetic energy. For a displacement of one step to the right from the initial position shown in Fig. 1 — the teeth of the first pole are aligned with the platen teeth — the right-side command coil must be excited in a way to concentrate the magnetic flux into pole 4. This brings about the flux density in this pole to a maximum, while in the other pole of the electromagnet (pole 3) the flux density is reduced to a negligible value. The mover will be driven to the right a quarter tooth-pitch (one step) and the pole 4 teeth will be aligned with the platen teeth.

For continuing the displacement to the right, coil 2 must be de-energized and the other one has to be excited. The developed force brings about the teeth of pole 2 in alignment with the platen teeth.

The above presented motor construction is not the only one possible, but it is the simplest one. This variant has some disadvantages, the most important being the fact that the produced thrusts at the outer and inner poles are not equal. This fact causes undesirable vibrations, which may be reduced by an adequate current control.

Balancing the advantages and the disadvantages of the permanent-magnet variable-reluctance linear motor one can say that this motor is a good one. It presents high tracking force to volume performance. It has the ability to hold fixed position under applied load and, moreover, it has high reliability and a very simple control system.

3. Motor model

The complex toothed configuration, the magnetic saturation of iron core parts and the permanent-magnet operating point change due to air-gap variable reluctance and control amperturns can be covered accurately by a *coupled circuit-field model*. The block diagram of the circuit-field model, composed of three main submodels, i.e. circuit, field and mechanical part, is given in Fig. 2.

The circuit-field model has been introduced in previous papers [4, 5, 6, 7] and all the characteristics of the motor, given here, are computed via this coupled model.

In order to obtain analytical results, which can be helpful in elaborating the control strategy, all the calculus must lay basically on three assumptions:

- the air-gap reluctances are much greater than all other reluctances, excepting of the permanent magnet;
- the permanent magnet reluctance is so great that no flux linkages produced by the currents which go through the control coils will pass from one side of the permanent magnet to the other side;
- the iron core parts of the motor magnetic circuit are not affected by saturation, so the superposition principle can be applied.

Hence, the equivalent magnetic circuit of the motor, when no control current occurs, is given in Fig. 3. If the coil number 2 is supplied, the flux produced by its current, Φ_c, can be obtained from the equivalent magnetic circuit given in Fig. 4.

All the computation is done supposing that the initial mover position is that one given in Fig. 1 and the mover's displacement is to the right, thus increasing the x-coordinate value. These initial conditions

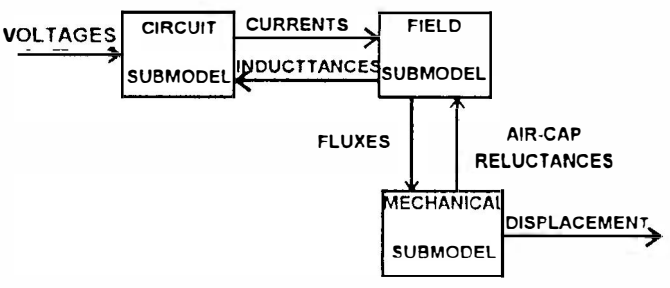

Fig. 2. Coupled circuit-field model of the permanent-magnet variable-reluctance linear motor.

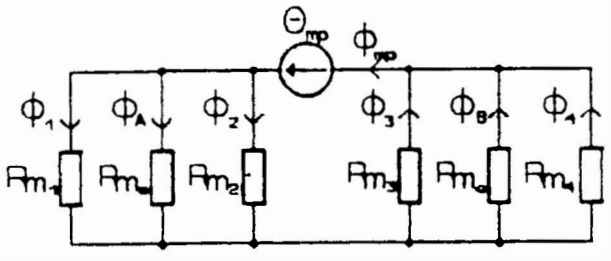

Fig. 3. Equivalent magnetic circuit of the motor with no-control m.m.f. (R_{me} - equivalent magnetic reluctance of one electromagnet).

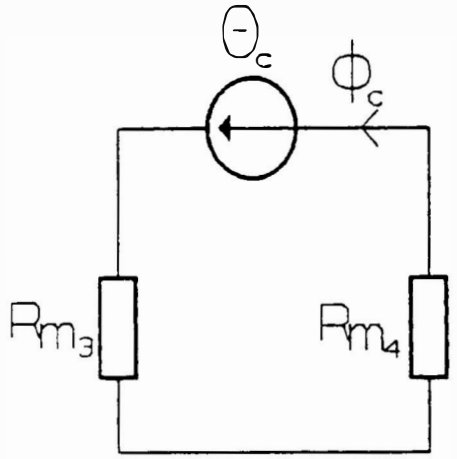

Fig. 4. Simplified equivalent magnetic circuit of the right-side electromagnet with control coil m.m.f.

does not affect the results and offer the possibilities to explain easier the motor's behavior and to simplify the mathematics.

The tangential force under one mover pole, j, is

$$F_{t_j} = -\left(\frac{\delta W_{m_j}}{\delta x}\right)\Big|_{\Phi_j = \text{ct.}} , \tag{1}$$

which means

$$F_{t_j} = -\frac{(N\Phi_j)^2}{2\mu_0 A}\,\frac{d\left[\delta_{e_j}(x)\right]}{dx} , \tag{2}$$

where the equivalent variable air-gap is, [4],

$$\delta_{e_j}(x) = \frac{2Z\delta'}{(2Z+\lambda-1)\left(1+a\cos\alpha_j\right)} \tag{3}$$

with

$$a = \frac{\lambda\left[1+\lambda\left(2Z-1\right)\right]}{2\left(2Z+\lambda-1\right)} . \tag{4}$$

If the equivalent magnetic permeance P_{m_e}, Fig. 3 [6], is

$$P_{m_e} = \frac{\mu_0 A}{Z\delta'}\left(2Z+\lambda-1\right), \tag{5}$$

after some computations expression (2) becomes

$$F_{t_j} = -\frac{\left(N\Phi_j\right)^2}{P_{m_e}}\,a\,\frac{2\pi}{t_d}\,\frac{\sin\alpha_j}{\left(1+a\cos\alpha_j\right)^2} , \tag{6}$$

where

$$\alpha = x\,\frac{2\pi}{t_d} \tag{7}$$

and

$$\alpha_1 = \alpha,\ \alpha_2 = \alpha+\pi,\ \alpha_3 = \alpha+\frac{\pi}{2},\ \alpha_4 = \alpha-\frac{\pi}{2} . \tag{8}$$

Considering the equivalent circuit given in Fig. 3, the fluxes under the poles, without excitation currents, are [6]

$$\Phi_j = \frac{\Theta_{MP} P_{m_e}}{4}\left(1+a\cos\alpha_j\right),\ \ j = 1\div 4. \tag{9}$$

The flux Φ_C is (Fig. 4)

$$\Phi_C = \frac{\Theta_C P_{m_e}}{4}\left(1+a\cos\alpha_3\right)\left(1+a\cos\alpha_4\right) \tag{10}$$

and, if the senses are that given in Figs. 3 and 4,

$$\Phi_{3r} = \Phi_3 - \Phi_C ,\ \ \Phi_{4r} = \Phi_4 + \Phi_C , \tag{11}$$

which leads to

$$\Phi_{3r} = \frac{\Theta_{MP} P_{m_e}}{4}\left(1+a\cos\alpha_3\right)\left[1-k_i\left(1+a\cos\alpha_4\right)\right] \tag{12}$$

$$\Phi_{4r} = \frac{\Theta_{MP} P_{m_e}}{4}\left(1+a\cos\alpha_4\right)\left[1+k_i\left(1+a\cos\alpha_3\right)\right] \tag{13}$$

with $\quad k_i = \dfrac{\Theta_C}{\Theta_{MP}} . \tag{14}$

The tangential forces produced under the mover's poles are

$$\begin{aligned} F_{t_1} &= -K_F \sin\alpha_1 , \\ F_{t_2} &= -K_F \sin\alpha_2 , \\ F_{t_3} &= -K_F\left[1-k_i-k_i\,a\cos\alpha_4\right]^2 \sin\alpha_3 , \\ F_{t_4} &= -K_F\left[1+k_i+k_i\,a\cos\alpha_3\right]^2 \sin\alpha_4 , \end{aligned} \tag{15}$$

with the force constant

$$K_F = \left(\frac{N\Theta_{MP}}{4}\right)^2 P_{m_e}\,a\,\frac{2\pi}{t_d} . \tag{16}$$

The resultant tangential force is

$$F_t = 4K_F k_i\cos\alpha\left(1-k_i\,a\sin\alpha\right) . \tag{17}$$

As it was proved in a previous paper [6], the induced e.m.f. in the non-supplied coil depends on the flux linkages through the external pole, here pole 1, and it is

$$e_1 = K_E \nu \sin\alpha \ , \tag{18}$$

where

$$K_E = \frac{2\pi}{t_d} N \frac{\Theta_{MP} P_{m_e}}{4} a \tag{19}$$

and

$$\nu = \frac{dx}{dt} \tag{20}$$

denotes the mover's velocity.

The induced e.m.f. in the supplied coil, here coil 2, is given by the variation of the flux linkages through the external pole, Φ_{4r}, and it is

$$e_2 = K_E \nu \cos\alpha \left(1 - 2 a k_i \sin\alpha\right) - \\ - \frac{K_E}{a} \frac{dk_i}{dt} \left(1 - a^2 \sin^2\alpha\right) . \tag{21}$$

The voltages equation written on the coil 2 is

$$u_2 = R i_2 + e_2 \tag{22}$$

which means that by knowing u_2 and i_2, the e.m.f. e_2 can be calculated as

$$e_2 = u_2 - R i_2 \tag{23}$$

In the Eq.(21), since $a<1$ (as one can see from the given example)

$$a^2 \sin^2\alpha < 1 \ , \tag{24}$$

$$e_2 + \frac{K_E}{a} \frac{N}{\Theta_{MP}} \frac{di_2}{dt} = K_E \nu \cos\alpha \left(1 - 2 a k_i \sin\alpha\right) \tag{25}$$

and

$$u_2 - R i_2 + \frac{K_E}{a} \frac{N}{\Theta_{MP}} \frac{di_2}{dt} = K_E \nu \cos\alpha \left(1 - 2 a k_i \sin\alpha\right) \tag{26}$$

With Eqs. (18) and (26) one can calculate the velocity ν and the position α of the mover, if k_i is considered constant and given by its average value.

4. Motor control

The control of the mover has to assure the imposed velocity profile and the positioning precision. Mover's speed is depending on the resulting tangential force and, therefore, the control has to act on the mover position α and, eventually, on the coil currents. Let discuss these aspects a little bit deeper.

It was stated that the m.m.f. produced by the permanent-magnet changes itself as its operating point does, due to air-gap variable reluctances and control amperturns. As it was already proved [6], when the iron core is not saturated the global air-gap reluctance is constant. Also, if the saturation does not affect the iron core parts, the permanent-magnet magnetic reluctance is bigger than the equivalent magnetic reluctance calculated on external magnetic circuit, including air-gaps. Therefore the coil amperturns produce feeble or no-changes at all in permanent-magnet m.m.f., which can be considered constant.

As one can see from Eq.(17), the total tangential force depends on the control amperturns via the m.m.f.'s factor k_i. The total tangential force increases quite slow in function of m.m.f.'s factor k_i (Fig. 5) and the saturation effects come up more and more important.

It means that superposition does not cover acceptably the phenomena and also that, in fact, the total tangential force will decrease because of increasing the equivalent air-gap under the active pole 4. Therefore, it looks reasonable to keep the m.m.f.'s factor at an average value around unity, which means that the control amperturns will be quite equal to the permanent-magnet m.m.f.

Now the things come up much more clear. The permanent-magnet m.m.f. is constant. The control amperturns are quite constant and equal to permanent-magnet m.m.f. The tangential force is depending only on the mover's displacement α and, therefore, the control system has to assure the corresponding value for α. Just one thing remains to be clarified: which is the optimum value of the displacement α?

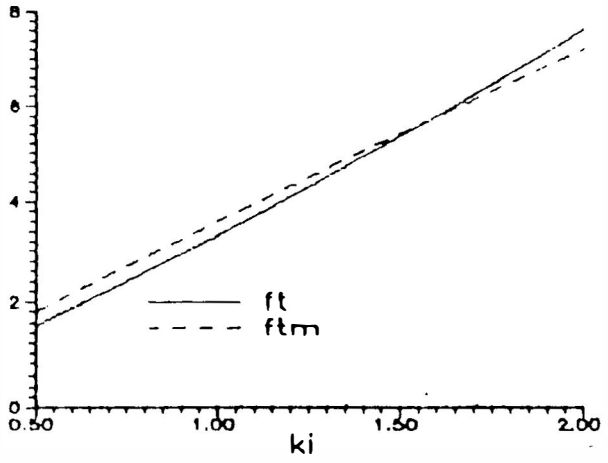

Fig. 5. Unitary total tangential (f_t) and average (f_{tm}) forces vs. m.m.f.'s factor k_i ($f_t = F_t / K_E$, $f_{tm} = F_{tm} / K_m$)

In order to determine this optimum α, the average force developed during one control step has to be considered, so

$$F_{t_m} = \frac{2}{\pi} \int_{\alpha_0}^{\alpha_0 + \frac{\pi}{2}} F_t \, d\alpha \ , \tag{27}$$

which gives

$$F_{t_m} = \frac{8}{\pi} K_F k_i \left(\cos \alpha_0 - \sin \alpha_0\right) \times \left[1 - \frac{k_i a}{2} \left(\sin \alpha_0 + \cos \alpha_0\right)\right] . \tag{28}$$

The optimum value of the displacement α is obtained from

$$\frac{d F_{t_m}}{d \alpha_0} = 0 , \tag{29}$$

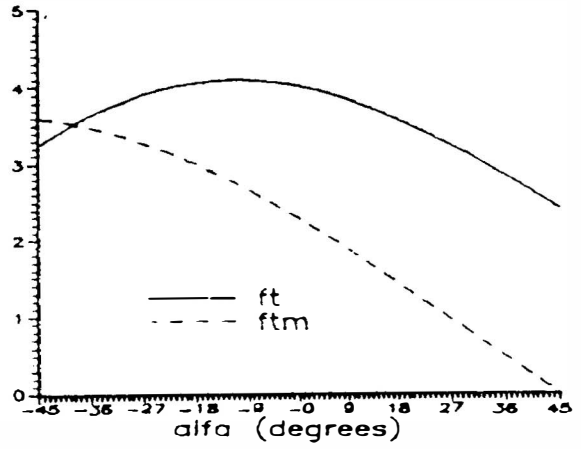

Fig. 6. Unitary total tangential (f_t) and average (f_{tm}) forces vs. control angle.

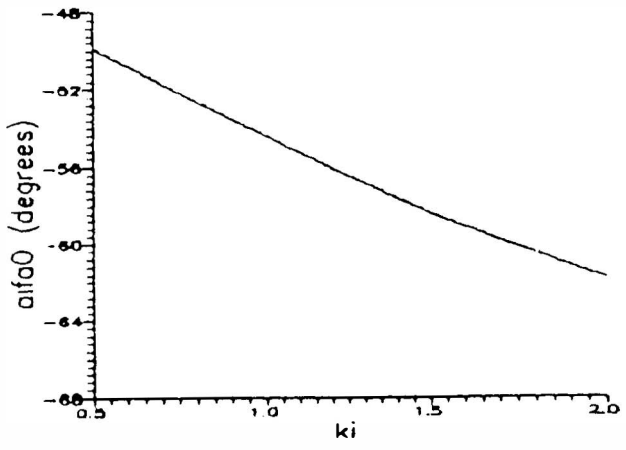

Fig. 7. Control angle α_0 as a function of m.m.f.'s factor k_i.

which leads to

$$\cos \alpha_0 + \sin \alpha_0 - 2 k_i a \sin \alpha_0 \cos \alpha_0 = 0 . \tag{30}$$

With motor constant a small enough, the optimum displacement becomes

$$\alpha_{0_0} = -\frac{\pi}{4} . \tag{31}$$

The forces variation in function of α and the α_0 variation in function of k_i are given in Figs. 6 and 7, respectively, in the case of the sample motor under consideration.

The motor control basics are already stated and even here it is no aim to introduce and detail a control system, the control strategy is almost obviously. The induced e.m.f. in the un-energized coil and in the supplied one can be monitored in order to determine the velocity and displacement. The controller has to assure a certain control current in order to obtain the imposed velocity. For high efficiency, the commutation of the command currents will be made at optimum control angle, which can be given as a function of coil current in the controller memory. So, the control angle will be always optimum and the developed tangential force will be controlled via coil currents. Sure, a special detection system of the mover position [2, 9] will simplify the computational procedure to be done through controller and will increase the precision, but will also increase the costs.

5. Results and conclusions

In order to sustain the theoretical results obtained on a simplified model of the permanent-magnet variable-reluctance linear motor, its characteristics are given by computer simulation via a coupled circuit-field model. This coupled model, presented by its components and connections in Fig. 2 [5, 7], starts from a very simple idea that all the motor characteristics can be calculated knowing the air-gap flux linkages. That is the field problem to be solved, to determine the flux linkages when the coil currents and permanent-magnet operating point are known. The combined circuit-field model is conceived to be solved by computer. The computational process consists of an iterative calculation, which allows us to take fully into consideration the iron parts magnetic saturation and permanent-magnet operating point changes due to air-gap permeances as functions of the mover-platen mutual position and control currents. The computer program based on this coupled circuit-field model offers the possibility to calculate all the motor characteristics, such as: forces, acceleration, velocity, displacement, control current, back e.m.f. etc.

The geometrical dimensions and parameters of the four-pole variable-reluctance permanent-magnet linear motor under consideration are given below:

- tooth width 1 mm
- slot width 1 mm
- tooth pitch (t_d) 2 mm
- no. of teeth per pole (Z) 5
- airgap (δ) 0.1 mm
- permanent magnet type VACOMAX-145
- residual flux density 0.9 T
- coercive force 650 KA/m.
- no. of coil turns 200
- coil resistance 3.5 Ω
- pole area 760 mm^2
- motor width 40 mm
- coefficient of equivalent air-gap permeance (λ) 0.672
- motor's constant (a) 0.244

In order to emphasize the differences which exist between open-loop and closed-loop driving modes, the motor total tangential force, velocity and displacement, plotted against time, are given under the same conditions. It means that in all situations the load is the same, there is no current control ($k_i \cong 1$) and the run time is 25 ms.

In Fig. 8, the open-loop drive-mode results are presented, the input frequency being constant and equal to 50 Hz. It is easy to see that, at the beginning, everything goes well, the total tangential force has great values, the velocity and displacement are

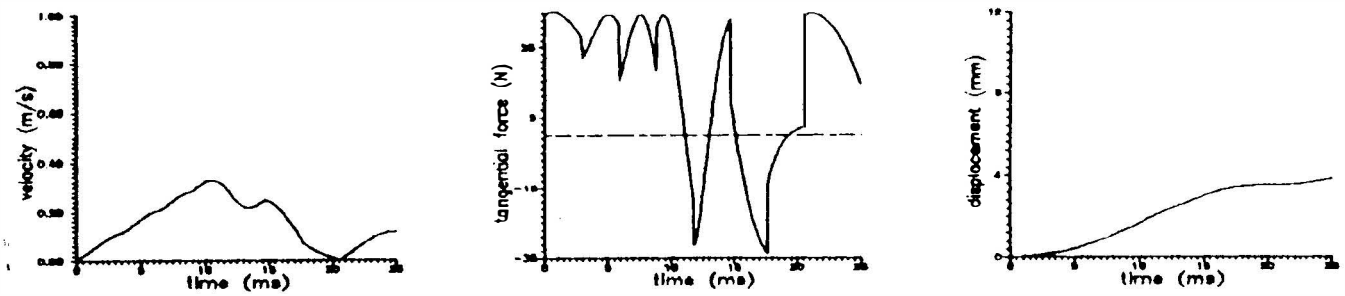

Fig. 8. Velocity, total tangential force and displacement as time functions in the open-loop drive mode.

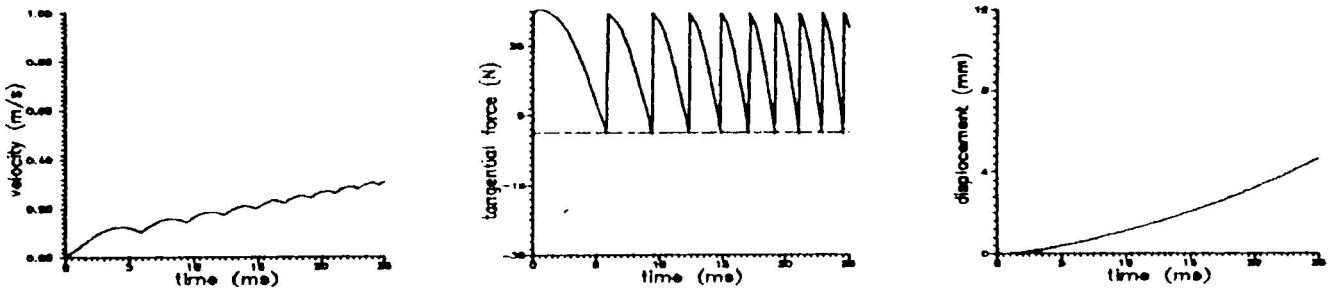

Fig. 9. Velocity, total tangential force and displacement as time functions in the closed-loop drive mode, for $\alpha_0 = 0$.

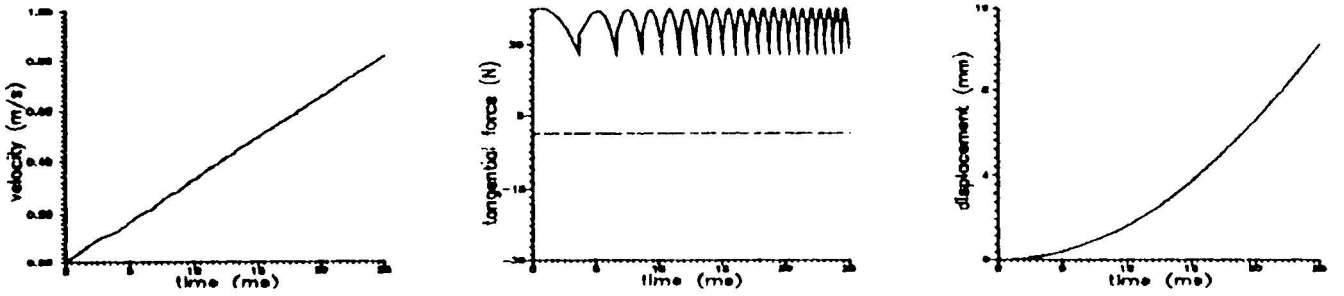

Fig. 10. Velocity, total tangential force and displacement as time functions in the closed-loop drive mode, for $\alpha_0 = -\pi/4$.

increasing quite uniformly. But, at a certain moment, because of velocity increasing, the control angle gets out of range and the force becomes negative. Now the synchronism is lost and the velocity comes to zero. Of course, there is a possibility to find a certain frequency in order to obtain an improving in motor characteristics, but it is not a valuable solution because it will work just with a certain load and control current value. Therefore, it is clear that the open-loop drive mode does not satisfy the conditions imposed by a high-precision system.

Figs. 9 and 10 contain the same characteris- tics of the motor operating in closed-loop mode, with the control angle value 0, respectively $-\pi/4$. If the control angle α is zero, the total tangential force has no negative values and the commutation moment takes place at zero value of the force. The force ripples are the greatest possible in closed-loop drive mode and, because of a smaller average value of the tangential force, the velocity increases slowly.

In the last Fig. 10 ($\alpha = -\pi/4$) the force's ripples are much smaller, the average value of the tangential force greater and the velocity increases pretty fast.

Some computed values obtained by motor simulation, which can be also found in the plots, are given in Table 1.

Table 1.

CONTROL METHOD	OPEN-LOOP	CLOSED-LOOP	
		$\alpha_0 = 0$	$\alpha_0 = -\pi/4$
max. tang. force [N]	35.46	35.46	35.46
min. tang. force [N]	-34.55	-0.75	21.78
max. velocity [m/s]	0.33	0.48	0.87
average tang. force [N]	3.31	19.92	31.15
average velocity [m/s]	0.05	0.33	0.59
final displacement [mm]	4.11	4.63	12.02

The motor given characteristics, obtained via computer simulation, stand by to sustain the theoretical results and to confirm that the control strategy has to be the one which comes up quite freely from the theory. That means, commutation at the optimum value of the control angle and velocity control via coil's current. It looks simple and very efficient.

List of main symbols

A mover pole area [m^2]
a motor constant
e_1, e_2 induced e.m.f. [V]
F_t resultant tangential force [N]
F_{t_j} tangential force ($j=1\div4$) [N]
F_{t_m} average tangential force [N]
i_2 coil 2 current [A]
j pole number
k_c Carter's factor
k_F tangential force coefficient
k_E induced e.m.f. coefficient
k_i m.m.f.'s factor (Θ_c / Θ_{MP})
N coil turns number
P_{m_e} equivalent magnetic permeance [H]
R control coil resistance [Ω]
R_m magnetic reluctance [1/H]
t time [s]
t_d mover's tooth-pitch [m]
u_2 coil number two supplying voltage [V]
v mover's velocity [m/s]
Z mover's pole teeth number
x horizontal coordinate (displacement) [m]
W_{m_j} magnetic energy under pole j ($j=1\div4$) [Ws]
α_j angular displacement ($j=1\div4$) [rad]
α_0 optimum angular displacement [rad]
δ motor air-gap [m]
δ' equivalent air-gap ($\delta' = k_c \delta$) [m]
δ_e equivalent variable air-gap [m]
λ coefficient of equivalent air-gap permeance
ϕ_c, ϕ_j, ϕ_{3r}, ϕ_{4r} flux linkages [Wb]
μ_0 magnetic constant ($\mu_0=4\pi/10^7$) [H/m]

References

1. Fu, Z.X., Nasar, S.A., Analysis of a hybrid linear stepper motor, *Proceedings of the Annual Symposium on Incremental Motion Control Systems & Devices* 1992, pp. 234-240.
2. Szabo, L., Viorel, I.A., Kovacs, Z., Variable speed conveyer system using e.m.f. sensing controlled linear stepper motor, *Proc. PCIM Conf.*, Nurnberg 1994; vol. Intelligent Motion, pp.183-190.
3. Veignat, N., Simon-Vermot M. - Karmous, M., Stepper motors optimization Use, *Proc. Int. Conf. on Electrical Machines*, Paris 1994, vol. 2., pp. 13-16.
4. Viorel, I.A., Topa, M., Kovacs, Z.,: Variable reluctance linear motor air-gap permeance calculations (in Romanian), *Scientific Bulletin of the Polytechnic Institute of Cluj-Napoca*, 27, (1984)., pp. 27-32.
5. Viorel, I.A., Kovacs, Z., Szabo, L., Sawyer type linear motor modelling, *Proc. Int. Conf. on Electrical Machines*, Manchester 1992, vol. II, pp. 697-701.
6. Viorel, I.A., Szabo, L., Kovacs, Z., Quadrature field-oriented control of a linear stepper motor, *Proc. PCIM Conf.*, Nurnberg 1993, vol. Intelligent Motion, pp. 64-73.
7. Viorel, I.A., Kovacs, Z., Szabo, L., Hybrid linear stepper motors. To appear in *Revue Roumaine des Sciences Techniques, Serie d'Electrotechnique et d'Energetique*.
8. Wendorff, E., Kallenbach, E., Direct drives for positioning tasks based on hybrid stepper motors, *Proc. PCIM Conf.*, Nurnberg 1993, vol. Intelligent Motion, pp. 38-52.
9. Xu, S., Hu, Y., Adaptive control of linear stepping motor, *Proc. Int. Conf. on Electrical Machines*, Paris, 1994, vol. 2., pp. 178-181.

Prof. Ioan-Adrian Viorel

Dipl. Ing. Lorand Szabo

Faculty of Electrical Engineering
Technical University of Cluj-Napoca
G. Baritiu str., 26-28
RO - 3400-Cluj-Napoca, Romania